2014

Effects of Vapor Injected Compression, Hybrid Evaporator Flow Control, and Other Parameters on Seasonal Energy Efficiency.

Christian K. Bach
Purdue University in West Lafayette, United States of America, bachc@purdue.edu

Eckhard A. Groll
Purdue University in West Lafayette, United States of America, groll@purdue.edu

James E. Braun
Purdue University in West Lafayette, United States of America, jbraun@purdue.edu

W. Travis Horton
Purdue University in West Lafayette, United States of America, wthorton@purdue.edu

Effects of Vapor Injected Compression, Hybrid Evaporator Flow Control, and Other Parameters on Seasonal Energy Efficiency.

Christian K. Bach
Purdue University in West Lafayette, United States of America, bachc@purdue.edu

Eckhard A. Groll
Purdue University in West Lafayette, United States of America, groll@purdue.edu

James E. Braun
Purdue University in West Lafayette, United States of America, jbraun@purdue.edu

W. Travis Horton
Purdue University in West Lafayette, United States of America, wthorton@purdue.edu

Effects of Vapor Injected Compression, Hybrid Evaporator Flow Control, and Other Parameters on Seasonal Energy Efficiency.

Christian K. BACH[*,1], Eckhard A. GROLL[2],
James E. BRAUN[3], W. Travis HORTON[4],

Purdue University Herrick Laboratories
140 S. Martin Jischke Dr.
West Lafayette, IN 47907
USA

[*,1]bachc@purdue.edu, [2]groll@purdue.edu,
[3]jbraun@purdue.edu, [4]wthorton@purdue.edu

* Corresponding Author

ABSTRACT

A companion paper (Bach et al. 2014) experimentally investigated the effects of vapor injected compression and hybrid evaporator flow control on capacity and COP. The goal of this paper is to provide insight into the effects of these technologies on heating seasonal performance (HSPF). HSPF was calculated using a modified version of the ANSI/AHRI 210/240 method, and parametric studies were performed to better understand the seasonal performance with a focus on comparing vapor injected and single stage system configuration. It was found that part load degradation and reduced capacity at low ambient temperature are factors that can degrade the seasonal performance. The increase in heat pump COP for the vapor injected configuration leads to only a small benefit - the main contributor to the increased HSPF of the vapor injected system configuration is its increased capacity towards low ambient temperatures.

1. INTRODUCTION

Hutzel and Groll (2013) investigated a 2-stage heat pump (HP) using simulations and experiments and reported seasonal energy efficiency based on a transient model for the entire year. They predicted a seasonal performance factor (HSPF) of 12.8 BTU/W-hr for the simulation based model and 7.7 BTU/W-hr based on curve fits to the in-field system data. A larger electricity consumption and lower COP during the colder months of the year was reported. The experimental setup had several issues, which contributed to the low seasonal performance.

Ramaraj (2012) investigated liquid flooded compression with regeneration as well as dual port vapor injected compression, with a focus on compressor testing. She conducted a simple bin-type analysis of these technologies for Minneapolis temperature data and predicted a 21% improvement in HSPF for the vapor injected system as well as a 34% improvement for the liquid flooded compression system. One contributor to the large predicted improvement is a relatively high cutout temperature of -10°C for the baseline single stage system as well as fixed pinch-point temperature and heat exchanger air inlet temperature differences.

Both, Hutzel and Groll (2013) and Ramaraj (2013) did not report the seasonal split between compressor energy consumption and auxiliary electric heat. Shen et al. (2014) numerically investigated sixteen different design options for cold climates and their effects on seasonal performance. They found that overcapacity, e.g. excess capacity at high ambient temperature, is the key to good seasonal performance and more important than other system improvements. His statement intuitively makes sense, since even at low ambient temperatures; the HP COP exceeds 1 but the system COP is moved towards 1 if insufficient HP capacity needs to be met by auxiliary electric heat. They furthermore found that oversizing a HP can lead to larger energy savings in less energy efficient buildings.

However, they pointed out that in warmer climate zones, a tradeoff between cyclic losses and resistance heat needs to be made. They used a design point of 47°F (8.3°C), and showed an increase in the use of resistive auxiliary heat in colder locations.

One issue that is often overlooked is the effect of external static pressure on heating mode COP. The rating standard (ANSI/AHRI 210/240, 2008) specifies an external static pressure of at least 50 Pa or 0.2 inches of water column ("WC) for heating mode performance rating. Proctor (2011), however found this to be unrealistically low. His survey of residential homes revealed that this value was always exceeded, and in some cases a static pressure of more than 1'' WC (or 5 times the minimum value of the rating standard) was observed. The average heating mode external static pressure from his data is approximately 0.75'' WC – which is still nearly 4 times as much as specified in the rating standard. Since this leads to higher indoor fan power consumption, a reduction in HSPF will occur.

This paper aims at investigating the effects of indoor fan power consumption, system level improvements, low temperature cutout temperature and other parameters on the HSPF of heat pumps using parametric studies. These parametric studies are simultaneously used to investigate the potential performance improvement of dual port vapor injected compression.

2. HSPF CALCULATION METHOD

This paper employs a modified version of the HSPF calculation method defined in ANSI/AHRI 210/240 (ANSI/AHRI, 2008). This method is equivalent to a bin-type method with the following aspects:

- Consideration of auxiliary electric heat below the balance point between heat pump capacity and building heating requirement (HP BP).
- Consideration of part load degradation, between HP BP and balance point between building and environment (BE BP), based on the excess capacity of the heat pump relative to the building. The amount of part load degradation can be adjusted using the cyclic degradation coefficient, with the default value of 0.25 leading to an increase in HP power consumption of 25% relative to the mapped HP performance in the limiting case of the BE BP, where the heating load reaches 0.
- Consideration of low temperature cutout (not considered for most parts of this study).
- Capacity and power consumption of the HP are inter/extrapolated based on experimental data. The method was modified to directly take in the actual test point temperature rather than the test plan temperature. This step was taken to reduce the uncertainty associated with the extrapolation. Note that most of the power consumption of the HP falls within the range of the experimental data, as shown in section 3.
- Consideration of defrosts. Since the configuration of the system shown in the companion paper did not allow for defrost testing, this part of the standard was not included. Note that this is equivalent to assuming similar defrost energy consumption for the different system configurations and that the reported HSPF values in this paper are larger than if defrost energy consumption was considered.
- Addition of normalized Minneapolis TMY3 data (NREL, 2013) as an example for a cold climate location.
- The design heating requirement (DHR) was chosen to be 60.8 kBtu/hr for 14°F (-10°C), which is equivalent to the interpolated capacity of the baseline single stage system for that temperature.

The test data for the HSPF calculation is based on the data of a companion paper (Bach et al. 2014), and can also be found in tabular form in Bach (2014).

3. CAPACITY, COP, AND BUILDING HEATING REQUIREMENT

One of the main issues with vapor compression heat pump systems is that heating capacity degrades with decreasing ambient temperature, while the building heating requirement increases. Figure 1 shows the heating requirement and HP capacity for different HP configurations normalized by their capacity at the 14°F (-10°C) design point. The data for the single stage CEC system is from a single speed conventional heat pump (Groll et al., 2011). Note the discrepancy between the linearly decreasing building heating requirement and the nearly linearly increasing capacity of the single speed system. For an extremely cold ambient temperature of -24°F (-31°C), the building heating requirement increases to more than 1.7 times the design point capacity while the heat pump capacity drops to 40% of the original capacity. This corresponds to only 23% coverage of the heating requirement by the heat pump for that temperature as shown in Figure 2. Significant overcapacity occurs above the design point – leading to part load losses in field operation. The single stage DOE system is the single stage configuration described in the companion paper (Bach et al. 2014), and uses a reduction of compressor speed towards higher ambient temperatures. This reduces overcapacity at high ambient temperatures. Only a small increase in capacity can be observed towards lower ambient temperatures, since the compressor runs at its full frequency at the design point. The vapor injected opt. DOE system (vi opt.) is the vapor injected configuration shown in Bach et al. (2014), and operates with reduced compressor speeds beginning at ambient temperatures above 17°F (-8.3°C), while the compressor speed is increased to the maximum tested value of 70 Hz at -8.3°C and -17.8°C ambient temperature and kept at the same minimum allowable value of 40 Hz as for the baseline single stage DOE system for 8.3°C. The larger capacity of the vapor injected configuration leads to less loss of capacity below the HP BP; for the most extreme shown temperature of -31°C, 47% of the heating requirement is met by the heat pump as shown in Figure 2 (or more than double CEC coverage).

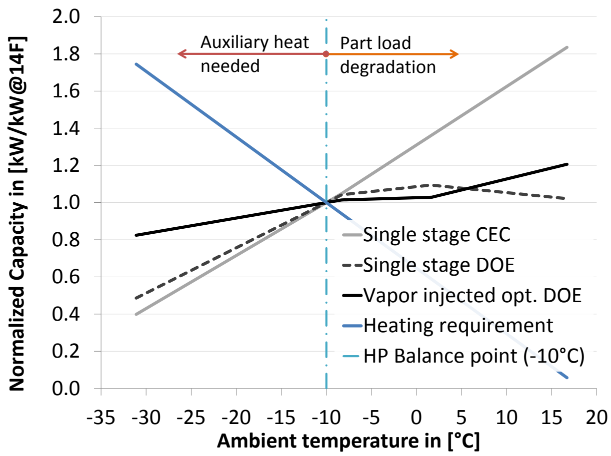

Figure 1: Normalized capacity and heating requirement relative to design point

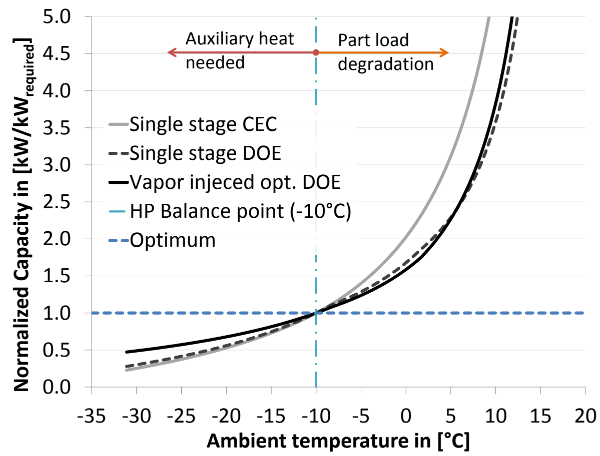

Figure 2: Normalized capacity relative to heating requirement

Figure 3 and Figure 4 show part load degradation factor as well as cumulative energy consumption for Minneapolis with the DOE baseline single stage and vapor injected configurations. Cumulative values are summed up from the lowest occurring temperature to the temperature of interest (T_n) shown on the x-axis, e.g. for a specified T_n, the cumulative value $X_{cum,n}$ is defined as a function of the ambient temperature bins sorted by increasing value, e.g.

$$X_{cum,n} = \sum_{k=0}^{n} X(T_k). \tag{1}$$

where X is a particular energy quantity (e.g., heating requirement) that is a function of T. The cumulative heating requirement is a result of the operating time at a certain bin temperature as well as of the heating requirement for that bin temperature. At very low temperatures, a high heating requirement occurs (see Figure 1) but there are only a few operating hours under these conditions. Therefore the slope of the curve is shallow. For high ambient temperatures, a low heating requirement and a large number of operating hours lead to a shallower slope. The slope of the heating requirement is steepest between the design point of -10°F and about 4°C. As a result of this, the cumulative compressor power consumption increases the quickest during that period as well.
The green markers in Figure 3 indicate the experimental data points. About 85% of the cumulative HP power consumption falls within that range of data and only 7% of the power consumption falls below the lower limit of that range. Auxiliary heat usage is most significant below -15°C. To the right of the HP BP, part load losses occur, most notably above -4°C. The total amount of part load losses is about half of the auxiliary heat power consumption. For the vi opt. configuration, Figure 4, 82% of the heat pump power consumption is located within the range of experimental data. The most notable improvement with the vi configuration is a lower heat pump balance point and a reduction of the auxiliary heat to nearly the same value as the part load losses. This reduction of auxiliary heat is the main contributor to the increase in HSPF.

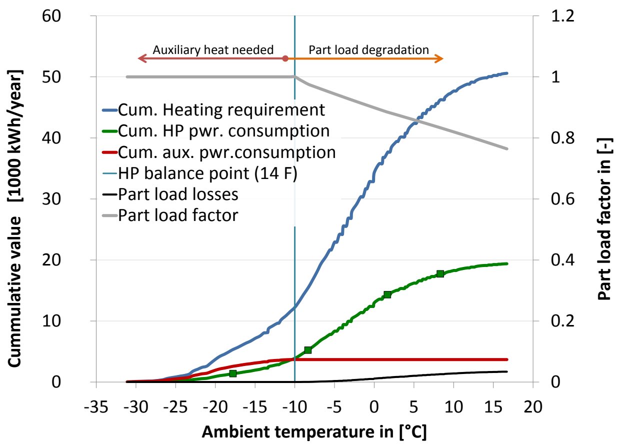

Figure 3: Cumulative values for heat pump and part load factor, DOE baseline single stage configuration (B0)

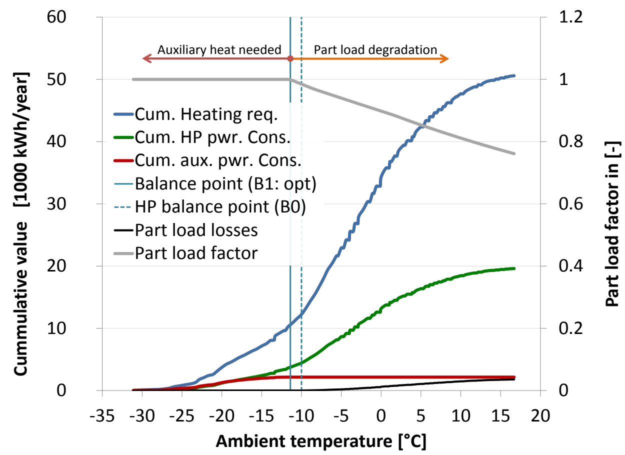

Figure 4: Cumulative values for heat pump and part load factor, DOE vapor injected opt. system (vi opt.)

2. RESULTS FOR DIFFERENT SYSTEM CONFIGURATIONS

6 different system configurations for the DOE heat pump were considered as shown in Table 1. Details on the system configurations along with system schematics can be found in the companion paper. The B0 configuration is used as the baseline, e.g. changes $\Delta X_{norm,i,j}$ in HSPF, auxiliary heat and HP power consumption are calculated for each system configuration *i* and climate region *j* as

$$\Delta X_{norm,i,j} = \frac{X_{i,j} - X_{baseline,j}}{X_{baseline,j}}. \tag{2}$$

Table 1: Input data used for different HSPF calculation cases

Configuration	*i*	Description
B0: single stage	1	Conventional single stage operation on variable speed drive
B1: match speed	2	Vapor injected compression, same compressor speed as for the single stage B0 but higher ambient humidity
B1: match speed, low humidity	3	Vapor injected compression, same compressor speed as for the single stage B0
B1H: match speed	4	Vapor injected compression, same compressor speed as for the single stage B0, hybrid evaporator flow control
B1: match capacity	5	Vapor injected compression, match capacity of B0 by decreasing compressor speed, except for H1 test.
B1: optimum	6	Full compressor speed at low ambient temperature HX test, reduced compressor speed for H3 and H2 test to match baseline capacity, and same compressor speed as baseline for high ambient temperature H1 test.

Figure 5 shows the HSPF for climate regions 4, 5, and Minneapolis for the different system configurations. The HSPF is higher for climate region 4, which is located south of climate region 5. The results for climate region 5 and Minneapolis are similar, since Minneapolis is located within region 5.

Figure 6 shows the HSPF improvement relative to B0, calculated by eqn. 2. The difference between the two B1 match speed configurations, which use a different set of outdoor air humidity, is very small for all climate zones. For conciseness, only the results for low humidity are shown. The configurations with same compressor speed as the baseline do not perform well in region 4 due to a larger operating time fraction under part load conditions. The B1H configuration leads to an improvement relative to the B1 match speed configurations. However, adjusting the compressor speed (B1 opt.) configuration leads to a even larger performance improvement due to less part load losses. The B1 match capacity case does not perform as good as the B1H and B1 opt configurations due to a smaller capacity at low ambient temperatures. The largest HSPF improvement of 6% for Minneapolis and 7% for region 5 is achieved with the B1 optimum configuration.

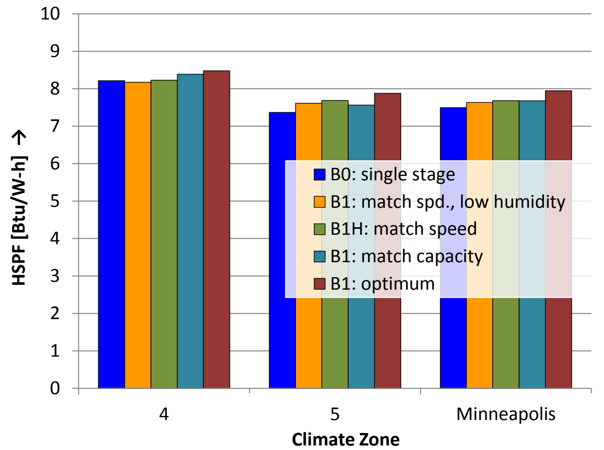

Figure 5: HSPF for different system configurations

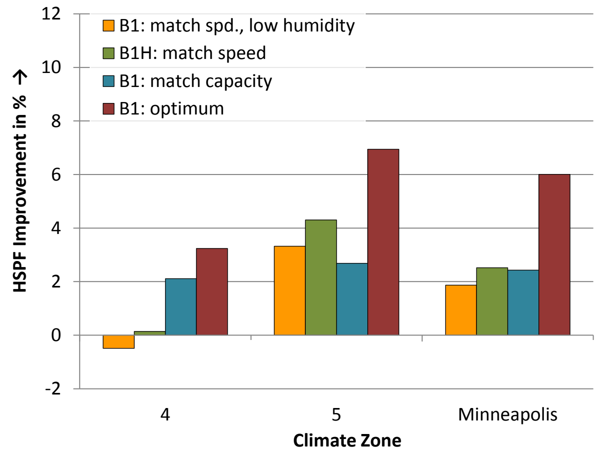

Figure 6: HSPF improvement relative to baseline B0

Figure 7 shows that the larger capacity of the vapor injected configurations (except for the B1 match capacity case) leads to a reduction of required auxiliary heat, here given normalized by the total power consumption of the baseline single stage system for each climate zone. The reduction in auxiliary heat energy consumption increases from the more southern climate zone *4* to the more northern climate zone *5.*
Figure 8 shows that the normalized HP power consumption increases by more than 3% for all considered climates with the exception of the B1 match capacity and opt. cases. The best trade-off between HP and auxiliary heat power consumption is achieved with the B1 opt case across all climate zones: a large reduction in auxiliary heat with a small increase in heat pump power consumption.

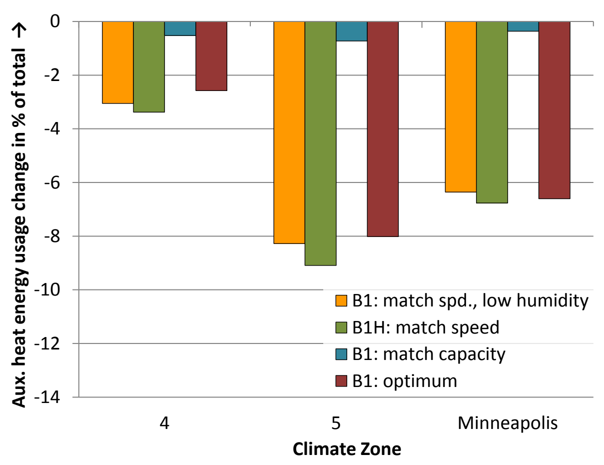

Figure 7: Auxiliary electric heat energy usage change relative to single stage baseline B0

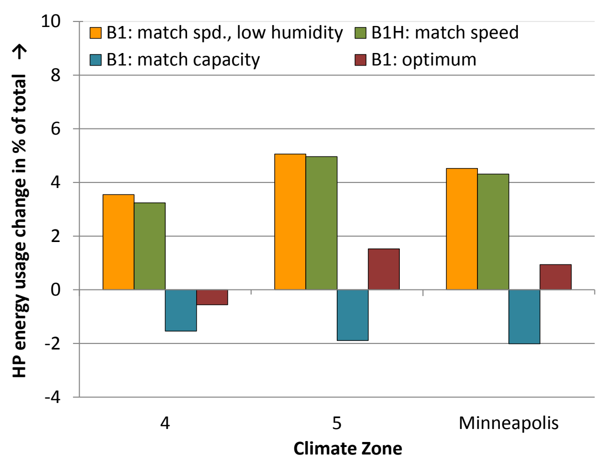

Figure 8: HP energy usage change relative to single stage baseline B0

5. PARAMETRIC STUDIES

Seasonal energy efficiency is dependent on multiple factors that are difficult to assess without the system actually being installed in a residential housing unit. These include the following factors:

- Sizing of heat pump relative to building – the sizing of the HP is most likely larger or smaller than the optimum.
- Part load degradation – dependent on the HP, the thermal response time of the building, and the sizing.
- Low ambient temperature cut out leading to 100% electric auxiliary heating under these conditions.
- External static pressure of duct system typically differs from the one employed in the rating standard.
- Local ambient temperature – affected by sunshine/shading. The general effect can be seen by using different climate zones as input, e.g. Figure 5.

To gain a general understanding on how these factors affect the seasonal performance, parametric studies were performed in this section. All studies in this section employ Minneapolis temperature data.

5.1 Design heating requirement and building balance point

The AHRI standard employs a design heating requirement at a design temperature together with a building balance point of 65°F (18.3°C) to linearly inter/extrapolate the heating requirement for each temperature bin. For the purpose of this paper, a design temperature of 14°F (-10°C) was chosen.

Figure 9 shows the effect of the design heating requirement on the HSPF. A design heating requirement of 15 kW leads to the optimum HSPF for both system configurations. A larger design heating requirement leads to performance degradation due to more auxiliary electric heat, and to the left of the optimum the effect of part load degradation becomes visible. Figure 10 shows the same results in terms of the balance point between heat pump and building, which is more intuitive to understand than the design heating requirement. The optimum heat pump balance point is around -15°C.

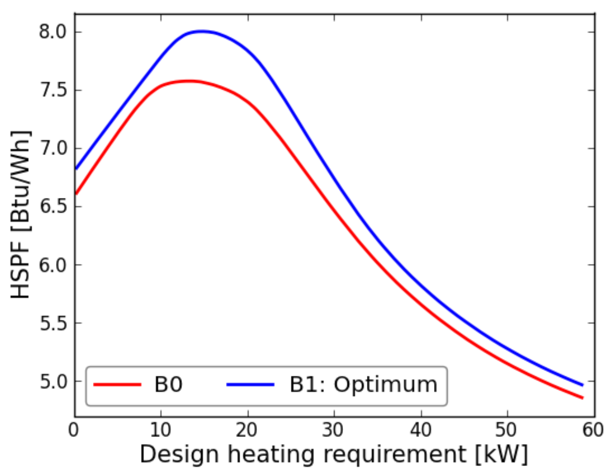

Figure 9: HSPF as a function of design heating requirement

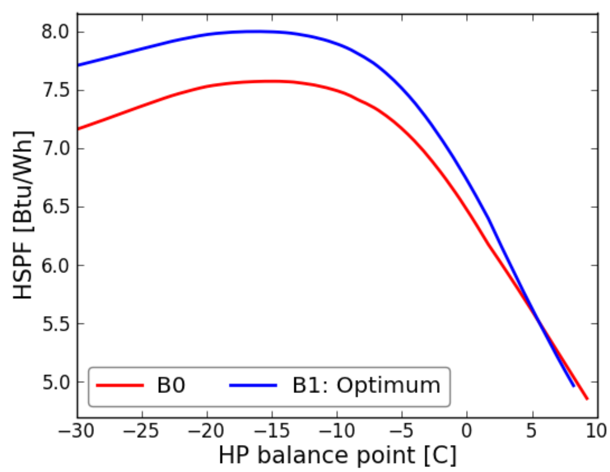

Figure 10: HSPF as a function of HP balance point

Figure 11 shows the annual share of the heating requirement as a function of the heat pump balance point (HP BP). For a HP BP of -23°C or less, most of the heating requirement is covered by the HP. At about 8.3°C, the HP and auxiliary heat share equal parts of the heating requirement. Figure 12 shows that this actually corresponds to about 70% of the electrical energy consumed by the auxiliary heat.

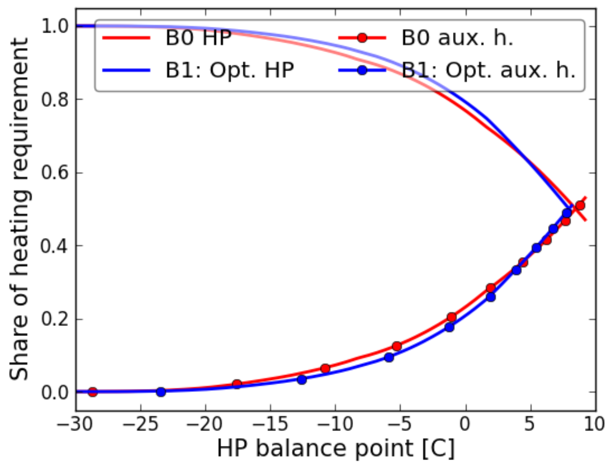

Figure 11: Share of annual heating requirement as a function of the HP balance point

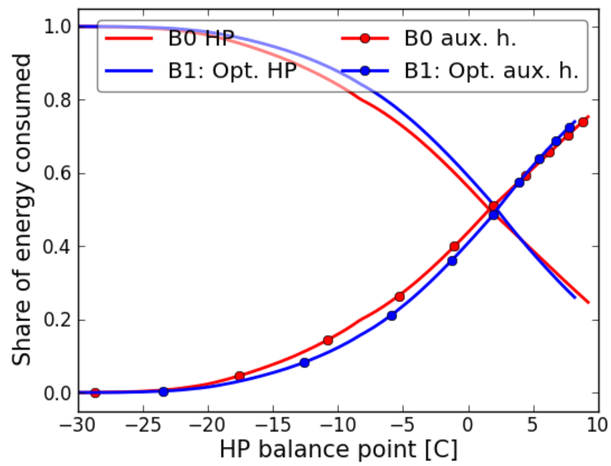

Figure 12: Share of electrical energy consumed as a function of the HP balance point

5.2 Part load/cyclic degradation

Cyclic degradation, e.g. cyclic operation of the heat pump to cover a heating requirement smaller than the heat pump capacity for a given temperature is captured by the AHRI 210/240 method by using a cyclic degradation coefficient. Figure 13 shows the influence of design heating requirement and cyclic degradation factor for heating (CDH) on the HSPF. A larger design heating requirement leads to a smaller influence of the CDH on the HSPF since the HP runs increasingly under full load conditions. For design heating requirements smaller than the 61 kBtu/hr chosen for the previously shown results, the influence of the CDH significantly increases. Figure 14 shows that this influence decreases the HSPF by nearly 2 points for a CDH of 0.3 and a HP balance point of -20 F. This BP is equivalent to coverage of nearly the entire heating requirement of Minneapolis by the heat pump.

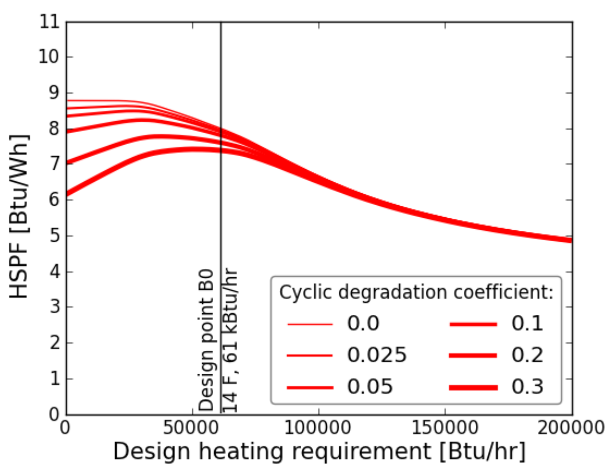

Figure 13: Influence of design heating requirement and cyclic degradation factor onto HSPF

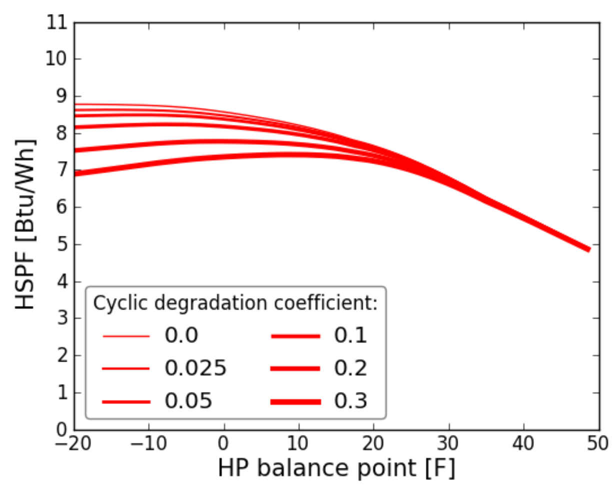

Figure 14: : Influence of heat pump balance point and cyclic degradation factor onto HSPF

5.3 External static pressure and fan power consumption

External static pressure can be significantly higher than specified in AHRI 210/240, as previously mentioned in the literature review. Figure 15 shows the power consumption and air flowrate for the employed indoor unit with a variable speed motor as a function of the external static pressure. The motor is programmed to keep the air flowrate constant over a wide range of external static pressures. Fan power consumption increases linearly between 50 and 250 Pa external pressure, while the air flowrate is approximately constant within that range. An external static pressure of 0.75"WC or 187 Pa leads to a fan power consumption of 609 W, which is 70% larger than the power consumption at the 50 Pa rating point. The air flowrate remains approximately constant up to that point; therefore

the taken test data can be modified to include the increased fan power consumption while assuming no change in condensing capacity of the HP. Figure 18 shows that the effect of increased external static on HSPF is relatively small: an external static pressure of 187 Pa only leads to a reduction of HSPF of 2% for the single stage system and 2.3% for the vapor injected system. Increased fan power shifts the HP BP only slightly and does not change the overall power consumption below the HP BP since it is merely a substitute for auxiliary electric heat in that case. Above the balance point it increases the HP capacity and also leads to an increase in overall power consumption. This leads to a smaller COP, which is additionally reduced by an increased part load factor.
Note that an increase in static pressure will lead to a more negative effect for AC systems, since the entire motor power consumption will need to be subtracted from the cooling capacity.

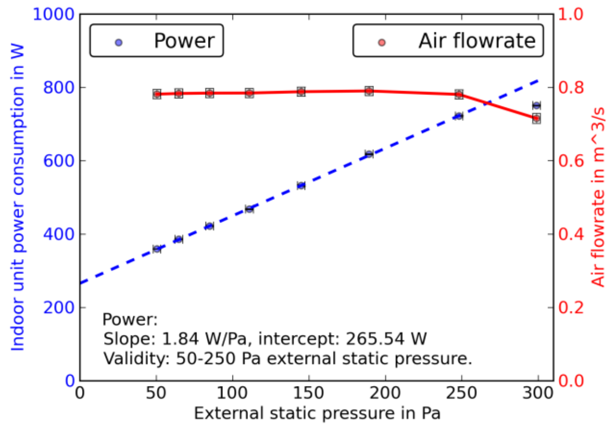

Figure 15: Indoor unit power consumption and flowrate as function of external static pressure for 40°C outlet temperature

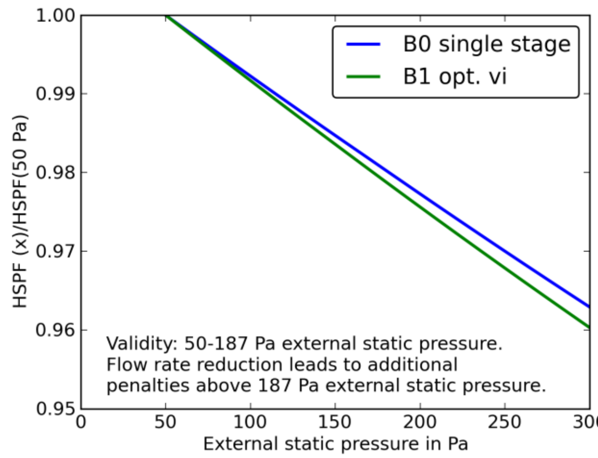

Figure 16: Influence of external static pressure onto HSPF, normalized by HSPF for 50 Pa external static

5.4 Low temperature cut out

A low temperature cutout is used to protect the system from excessive discharge temperatures, which would lead to degradation of the refrigerant oil and reduce system lifetime. The maximum allowable discharge temperature was assumed to be 135°C, which is the setpoint of the OEM discharge temperature switch. This value was not reached during clean coil tests – even at the lowest ambient temperature of -17.8°C. Therefore the actual cutout-temperature was estimated based on the results of all tests, including blocked coil tests and an assumed offset between ambient temperature and saturated suction temperature of 12 K. Figure 17 shows that the vapor injected system does not have any limitations due to low temperature cutout since the discharge temperature does not exceed 120°C, even for -28°C ambient temperature. The baseline system needs to be cut out for ambient temperatures below approximately -27°C. Figure 18 shows that this leads to an HSPF degradation of much less than 1%. Relying on the low pressure cutout switch of the HP would lead to a 3% reduction in HSPF while the -10°C cutout used in Ramaraj (2013) leads to a 16% HSPF reduction. Ramaraj (2013) used the same compressor as our setup but based the cutout temperature on the mapping of data from a compressor test stand and a simple cycle model. Both the higher ambient temperature during the testing and the simple cycle model with fixed pinch points and air-inlet temperature differences lead to an increase in discharge temperature when compared to our data.

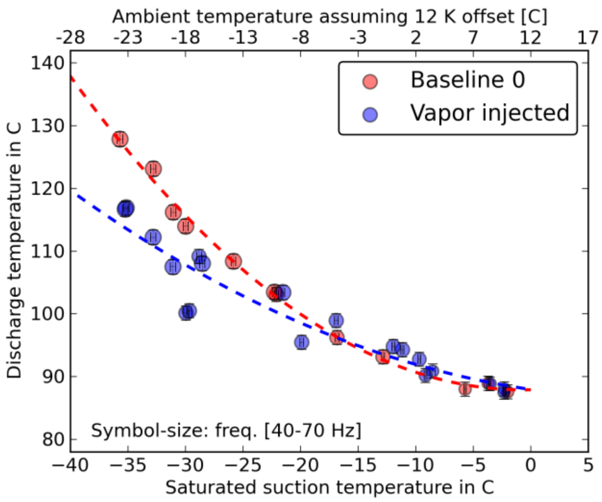

Figure 17: Discharge temperature as function of saturated suction temperature

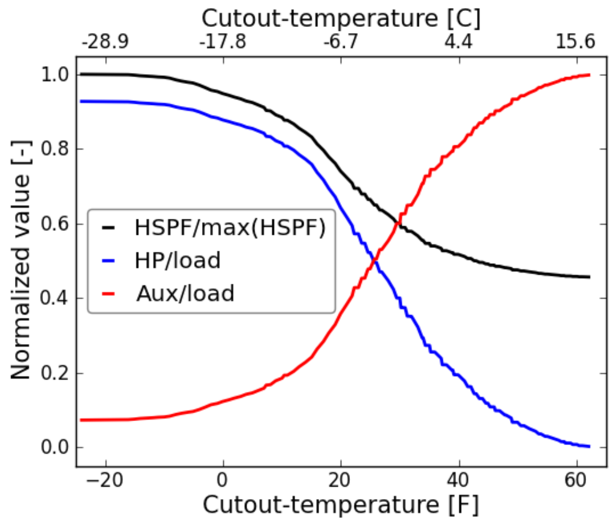

Figure 18: Normalized HSPF, share of HP and auxiliary heat power consumption as a function of cutout temperature, single stage B0 configuration

6. CONCLUSIONS

The following points summarize the findings of this paper:

- System capacity at low ambient temperatures is the most important factor for a high HSPF.
- Part load degradation sets the upper limit for larger system capacity, e.g. increasing the system size eventually leads to HSPF degradation if the HP runs in part-load for a large amount of operating time.
- Compressors with an extremely wide frequency range (e.g. 10-100 Hz) might be able to address the above issue and should therefore be investigated in future projects.
- The benefit of the vapor injected system is mainly is mainly the result of an increase in low ambient temperature capacity.
- Low ambient temperature cutout was found to be of no serious concern for the HSPF of the tested system - even for Minneapolis conditions.
- External static pressures as observed in practice do not lead to a large degradation of seasonal heating performance.

NOMENCLATURE

Δ	Difference	(kW) or (-)
X	Value placeholder	(kW) or (-)

Subscript

baseline	baseline single stage configuration
cum	cumulative
i	system configuration index
j	climate zone index
k	temperature bin index
n	maximum temperature bin index
norm	normalized

REFERENCES

AHRI (2008). ANSI/AHRI Standard 210/240 with Addendum 1 (Formerly ARI Standard 210/240), 2008, Standard for Performance Rating of Unitary Air-Conditioning & Air-Source Heat Pump Equipment.

Bach C. K., Vetsch, B., Groll, E. A., Braun, J. E., and Horton, W. T, (2014), Experimental Investigation of Vapor Injected Compression for Cold Climate Heat Pumps and its Effects on their Performance, *15th International Refrigeration and Air Conditioning Conference at Purdue*, West Lafayette.

Bach C. K. L, 2014, Refrigerant Side Compensation for Air-Side Maldistribution of Evaporators and its Effects on System Performance, *Dissertation*, Ray W. Herrick Laboratories, Purdue University, West Lafayette.

Groll, E. A., Braun, J. E., and Bach, C. K., 2011, Optimizing refrigerant distribution in evaporators - final report for California Energy Commission, final report, *Ray W. Herrick Laboratories*, Purdue University, West Lafayette.

Hutzel, W. J., and Groll, E.A., 2013, Air Source Cold Climate Heat Pump, ESTCP final project report EW-201136, *Purdue University*.

Proctor, J., Chitwood, R., and Wilcox, B. A., 2011, Efficiency Characteristics and Opportunities for New California Homes, *Proctor Engineering Group, Ltd*.

Ramaraj, S., 2013, Vapor Compression Cycle Enhancements for Cold Climate Heat Pumps, Master's thesis, *Purdue University Herrick Laboratories*.

Shen, B., Abdelaziz, O., and Rice, C. K., 2014, Compressor Selection and Equipment Sizing for Cold Climate Heat Pumps, 11th IEA Heat Pump Conference 2014, May 12-16 2014, *Canadian GeoExchange Coalition*, Montréal (Québec) Canada, Paper P.6.11.

NREL, 2013, National Solar Radiation Data Base - 1991- 2005 Update: Typical Meteorological Year 3 - List of Sites in Alphabetical Order by State and Site Name, location 726580, Minneapolis-St Paul Int'l Arp, downloaded 09/22/2013 from http://rredc.nrel.gov/solar/old_data/nsrdb/1991-2005/tmy3/by_state_and_city.html.

ACKNOWLEDGEMENT

We acknowledge the support of our sponsors and co-sponsors: the USDOE, Carrier Corporation and Emerson Climate technologies and particularly like to express our gratitude to Kok-Hiong Kee and Kirill Ignatiev. We also thank Bernhard Vetsch and Frank Lee for their help with this project.